



## Recyclable cell-surface chemical tags for repetitive cancer targeting

Rimsha Bhatta <sup>a,1</sup>, Joonsu Han <sup>a,1</sup>, Jingyi Zhou <sup>a</sup>, Haoyu Li <sup>a</sup>, Hua Wang <sup>a,b,c,d,e,f,g,\*</sup>

<sup>a</sup> Department of Materials Science and Engineering, University of Illinois at Urbana-Champaign, Urbana, IL 61801, USA

<sup>b</sup> Cancer Center at Illinois (CCIL), Urbana, IL 61801, USA

<sup>c</sup> Department of Bioengineering, University of Illinois at Urbana-Champaign, Urbana, IL 61801, USA

<sup>d</sup> Carle College of Medicine, University of Illinois at Urbana-Champaign, Urbana, IL 61801, USA

<sup>e</sup> Beckman Institute for Advanced Science and Technology, University of Illinois at Urbana-Champaign, Urbana, IL 61801, USA

<sup>f</sup> Materials Research Laboratory, University of Illinois at Urbana-Champaign, Urbana, IL 61801, USA

<sup>g</sup> Institute for Genomic Biology, University of Illinois at Urbana-Champaign, Urbana, IL 61801, USA



### ARTICLE INFO

#### Keywords:

Metabolic glycan labeling

Cell targeting

cancer

Click chemistry

Chemotherapy

### ABSTRACT

Metabolic glycan labeling provides a facile yet powerful tool to install chemical tags to the cell membrane via metabolic glycoengineering processes of unnatural sugars. These cell-surface chemical tags can then mediate targeted conjugation of therapeutic agents via efficient chemistries, which has been extensively explored for cancer-targeted treatment. However, the commonly used *in vivo* chemistries such as azide-cyclooctyne and tetrazine-cyclooctene chemistries only allow for one-time use of cell-surface chemical tags, posing a challenge for long-term, continuous cell targeting. Here we show that cell-surface ketone groups can be recycled back to the cell membrane after covalent conjugation with hydrazide-bearing molecules, enabling repetitive targeting of hydrazide-bearing agents. Upon conjugation to ketone-labeled cancer cells via a pH-responsive hydrazone linkage, Alexa Fluor 488-hydrazide became internalized and entered endosomes/lysosomes where ketone-sugars can be released and recycled. The recycled ketone groups could then mediate targeted conjugation of Alexa Fluor 647-hydrazide. We also showed that doxorubicin-hydrazide can be targeted to ketone-labeled cancer cells for enhanced cancer cell killing. This study validates the recyclability of cell-surface chemical tags for repetitive targeting of cancer cells with the use of a reversible chemistry, which will greatly facilitate future development of potent cancer-targeted therapies based on metabolic glycan labeling.

### 1. Introduction

Targeted delivery of therapeutics to tumors remains a crucial goal for the development of cancer therapies with improved efficacy and reduced off-target toxicity [1–3]. As an alternative to conventional antibody-based active targeting approaches that exploit cancer-overexpressed protein receptors [4,5], metabolic glycan labeling coupled with efficient click chemistry has emerged as a new active targeting strategy [6–8]. Unnatural monosaccharides bearing chemical tags can be metabolized by cancer cells via glycoengineering pathways and be expressed on the cell membrane in the form of glycoproteins and glycolipids [9–11]. These cell-surface chemical tags (azide, alkyne, etc.) can then mediate targeted conjugation of molecules of interest via efficient chemistries such as reagent-free click chemistry between azide and dibenzocyclooctyne (DBCO) [6,12,13]. The combination of metabolic

glycan labeling and click chemistry has been widely explored for tumor-targeted delivery of therapeutic agents [14–18]. In the first step, tumors are metabolically labeled with chemical tags (e.g., azido groups) via intratumoral injection of non-specific unnatural sugars [19,20], or intraperitoneal/intravenous injection of nanoparticles containing unnatural sugars [21–24], or intravenous injection of unnatural sugars that can preferentially label cancer cells [8,25]. In the second step, agents bearing the complementary functional group (e.g., DBCO) are administered to covalently conjugate to chemically tagged cancer cells. Due to the high density of installable chemical tags and high efficiency of click chemistries [8], this cancer-targeting approach has demonstrated great potential for developing efficacious targeted therapies. While significant progress has been made to improve the cancer-labeling efficiency and specificity of unnatural sugars, currently used *in vivo* biorthogonal chemistries have been limited to azide-cyclooctyne and tetrazine-

\* Corresponding author at: Department of Materials Science and Engineering, University of Illinois at Urbana-Champaign, Urbana, IL 61801, USA.

E-mail address: [huawang3@illinois.edu](mailto:huawang3@illinois.edu) (H. Wang).

<sup>1</sup> These authors contributed equally.

cyclooctene reactions [14].

Commonly-used bioorthogonal chemistries including azide-cyclooctyne and tetrazine-cyclooctene reactions only allow for one-time use of cell-surface chemical tags. For example, the cycloaddition of azide and DBCO forms a stable triazole ring structure that cannot be reversed. In contrast, endogenous cell-surface protein receptors are able to release bounded targeting ligands in endosomes and become recycled to the cell surface for continuous targeting [26–28]. The non-recyclability of cell-surface chemical tags prevents the repetitive targeting of extracellular cargos and limits the achievable anticancer efficacy. Indeed, upon the removal of unnatural sugars, the density of cell-surface chemical tags will decrease over time, especially when cells divide [11,14]. As a result, the targetable time window could be narrow and thus limits the design of cancer-targeted therapy over a longer course. To enable repetitive targeting, unnatural sugars have to be re-administered to introduce new chemical tags to cancer cell membranes [8,23]. These issues can be potentially addressed via the development of recyclable chemical tags. We previously showed that DBCO-

molecules covalently captured by azido-labeled cells were gradually internalized and entered endosomes [8]. In view of this, we hypothesize that unnatural sugars can be potentially recycled if the formed covalent bond between chemical tags and attached cargos can be cleaved in endosomes, resulting in the re-expression of chemical tags for subsequent repetitive targeting of cargos. Among the reversible chemistries responsive to cellular triggers such as low pH, reductives, and enzymes [29], hydrazide/ketone chemistry could be a good example to study as it can occur under physiological or mildly acidic conditions (pH = 7.4–6.5) while the formed hydrazone bond can be rapidly cleaved in acidic endosomes (pH = 5.0–6.0) [30–34]. Metabolic labeling of cells with ketone groups, together with covalent capture of hydrazide- or hydroxyamine-bearing molecules, has been achieved in the past [9–14]. However, the internalization pathway and intracellular fate of covalently conjugated molecules remain elusive, let alone the ability of cell-surface ketone groups to mediate repetitive targeting of hydrazide-bearing agents including therapeutics. In this study, by taking advantage of the pH-responsive hydrazide/ketone chemistry, we examined the

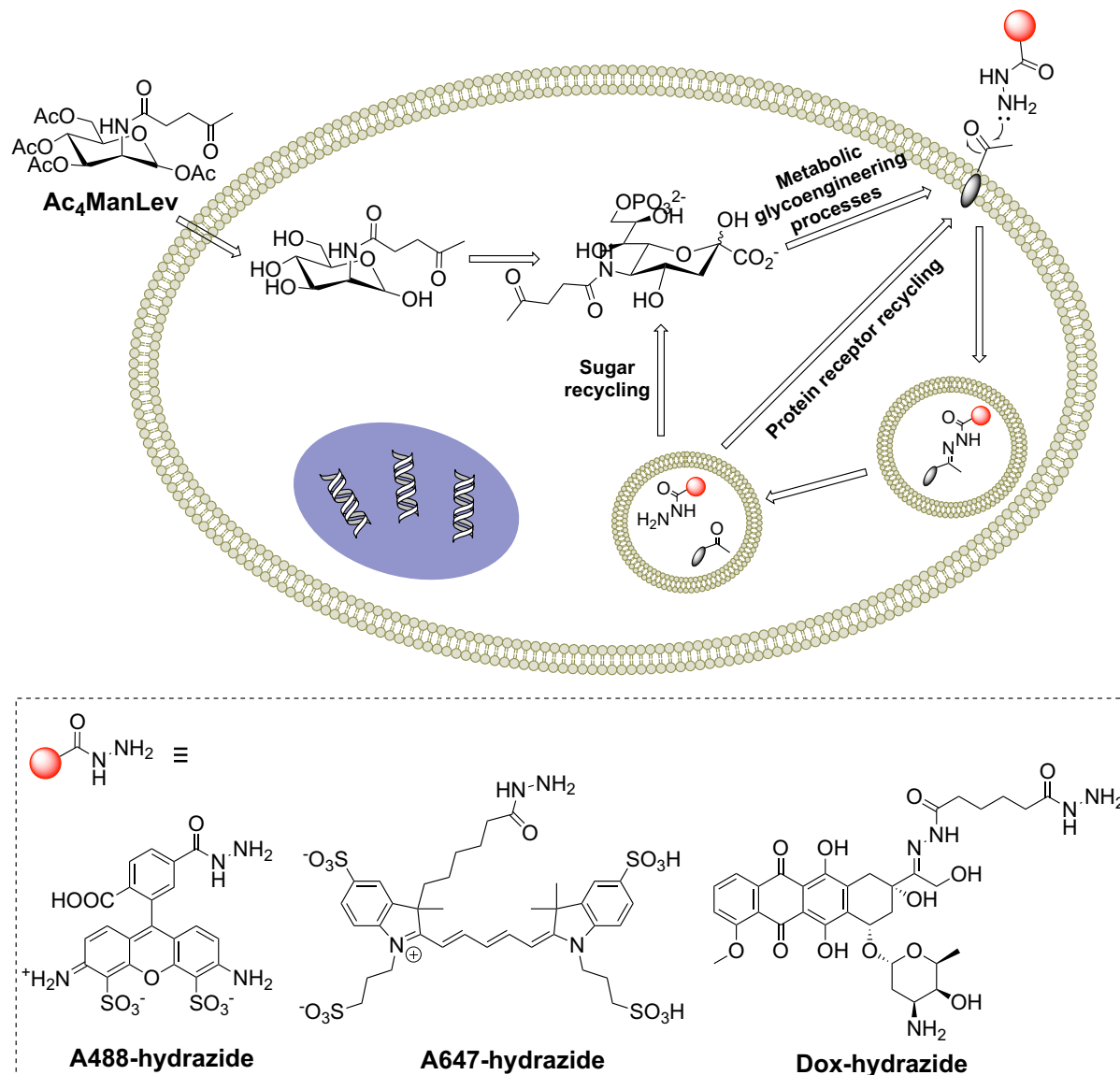


**Fig. 1.** Schematic illustration for metabolic labeling and repetitive targeting of cancer cells. Ac<sub>4</sub>ManLev can undergo the metabolic glycoengineering process and label cell-surface glycoproteins and glycolipids with ketone groups, which enable subsequent conjugation of hydrazide-bearing diagnostic and therapeutic agents, including A488-hydrazide, A647-hydrazide, and Dox-hydrazide. The formed conjugates become endocytosed and release ketone-labeled sugars and hydrazides in acidic endosomes. The resulting ketone-labeled sugars can then be recycled to cell membranes for continuous targeting of hydrazide-bearing agents.

covalent capture and internalization process of hydrazide-molecules by ketone-modified cancer cells and the recyclability of cell-surface ketone groups for repetitive targeting of extracellular cargo (Fig. 1). We further evaluated the targeted conjugation of hydrazide-bearing chemotherapeutics to ketone-labeled cancer cells for improved cancer killing.

## 2. Results and discussion

We first synthesized tetraacetyl-*N*-(levulinic acyl) mannosamine

(Ac<sub>4</sub>ManLev) as the potential metabolic labeling agent (Fig. 1). Compared to *N*-(levulinic acyl) mannosamine (ManLev) that was previously used for metabolic labeling of cells, Ac<sub>4</sub>ManLev potentially exhibits a higher cellular uptake rate and thus a higher labeling efficiency. The synthesized Ac<sub>4</sub>ManLev was characterized by <sup>1</sup>H NMR, <sup>13</sup>C NMR, and mass spectrometry (Fig. S1–3). A mixture of isomers ( $\alpha$  and  $\beta$ ) was detected by the <sup>1</sup>H NMR spectrum, but was indistinguishable in <sup>13</sup>C NMR (Fig. S1–2). To study whether Ac<sub>4</sub>ManLev can metabolically label cancer cells with ketone groups, LS174T colon cancer cells were incubated with

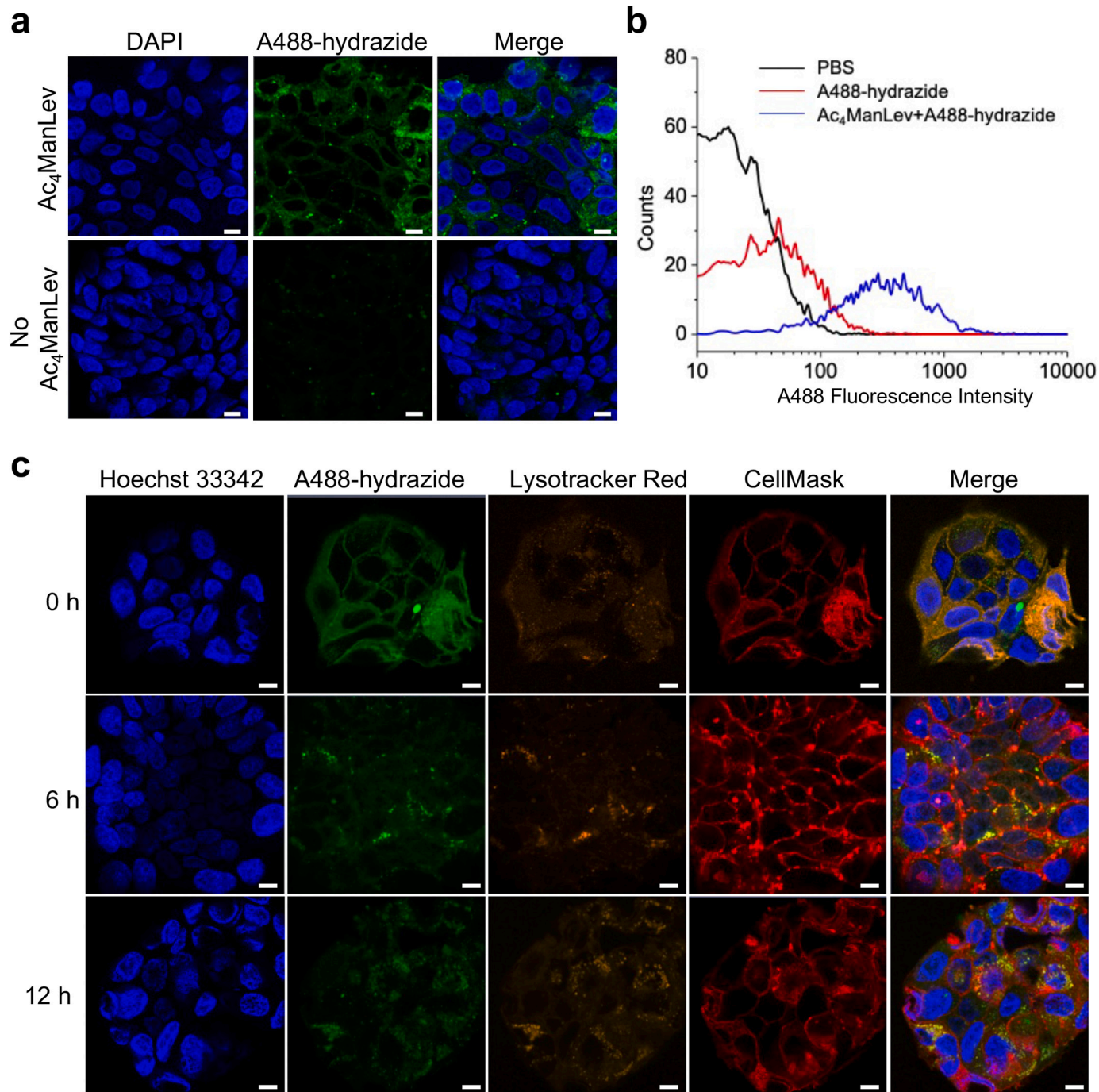


**Fig. 2.** Ac<sub>4</sub>ManLev-treated LS174T cells can covalently capture and internalize hydrazide-bearing molecules. (a) Confocal images of LS174T cells treated with Ac<sub>4</sub>ManLev or PBS for three days and incubated with A488-hydrazide for 30 min. Cell nuclei were stained with DAPI. Scale bar: 10  $\mu$ m. (b) Representative FACS plots of LS174T cells treated with Ac<sub>4</sub>ManLev or PBS for three days and incubated with A488-hydrazide for 30 min. (c) Confocal images of A488-hydrazide conjugated LS174T cells at 0, 6, and 12 h, respectively post transfer to fresh medium. Cells were treated with Ac<sub>4</sub>ManLev for three days and incubated with A488-hydrazide for 30 min. The cell nucleus, endosomes/lysosomes, and membrane were stained with Hoechst 33342 (blue), Lysotracker™ Red DND-99 (orange), and deep red Cell Mask (red), respectively. Scale bar: 10  $\mu$ m. (For interpretation of the references to colour in this figure legend, the reader is referred to the web version of this article.)

Ac<sub>4</sub>ManLev (100  $\mu$ M) for three days, followed by incubation with Alexa Fluor 488 (A488)-hydrazide for 30 min. Confocal images of LS174T cells treated with Ac<sub>4</sub>ManLev showed much higher A488 fluorescence intensity on the cell surface compared to control cells without Ac<sub>4</sub>ManLev treatment (Fig. 2a). Flow cytometry analysis also confirmed the much

stronger A488 fluorescence intensity in Ac<sub>4</sub>ManLev-treated LS174T cells than in non-treated cells (Fig. 2b). Similarly, a higher Alexa Fluor 647 (A647) fluorescence signal was detected in LS174T cells that were pre-treated with Ac<sub>4</sub>ManLev and then incubated with A647-hydrazide, in comparison to cells without Ac<sub>4</sub>ManLev pretreatment (Fig. S4). It is

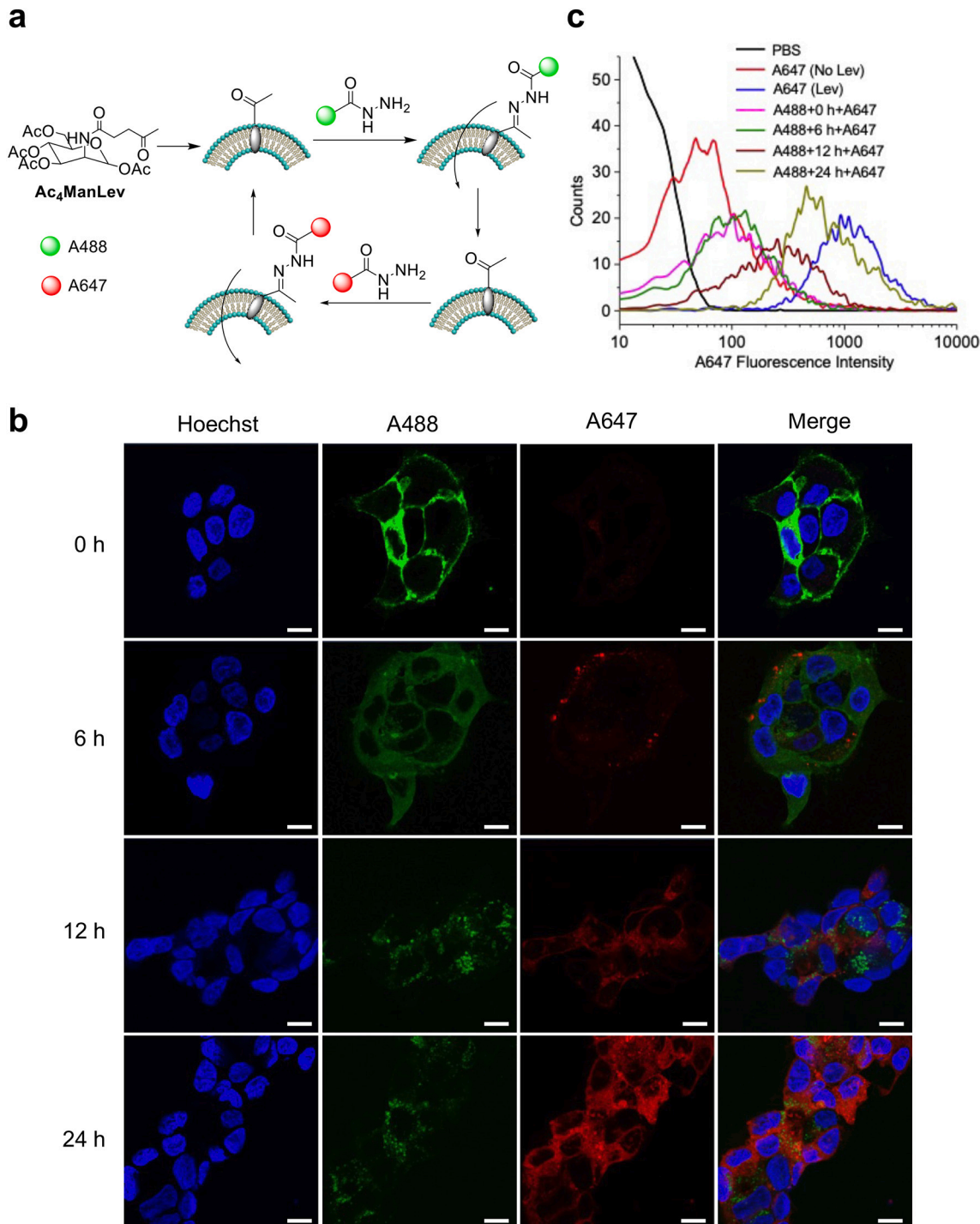


**Fig. 3.** Cell-surface ketone groups can be recycled after conjugation with A488-hydrazide, for subsequent targeting of A647-hydrazide. (a) Schematic illustration of recyclable cell-surface ketone groups for repetitive targeted conjugation of hydrazine-cargos. (b) Confocal images of LS174T cells after 1-h incubation with A647-hydrazide that was added at 0, 6, 12, and 24 h, respectively post covalent capture of A488-hydrazide. Cells were pretreated with Ac<sub>4</sub>ManLev (100  $\mu$ M) for three days and incubated with A488-hydrazide for 1 h. After A488-hydrazide conjugation, cells were transferred to fresh medium and further incubated for 0, 6, 12, or 24 h prior to the addition of A647-hydrazide. Cells were imaged after 1-h incubation with A647-hydrazide. Cell nuclei were stained with Hoechst 33342 (blue). Scale bar: 10  $\mu$ m. (c) Representative A647 histograms of LS174T cells following the same treatment as described in (b). Cells pretreated with PBS or A647-hydrazide only were used as negative controls. (For interpretation of the references to colour in this figure legend, the reader is referred to the web version of this article.)

noteworthy that the incubation of cancer cells with a much lower concentration of Ac<sub>4</sub>ManLev (50 or 100  $\mu$ M) was able to mediate significant targeting of A488-hydrazide or A647-hydrazide, compared to the previously reported use of millimolar ManLev [11]. These experiments demonstrated that Ac<sub>4</sub>ManLev can metabolically label LS174T cancer cells with ketone groups and that the cell-surface ketone groups can mediate the covalent conjugation of hydrazide-bearing molecules.

We next studied the cellular internalization process of covalently captured A488-hydrazide in ketone-labeled LS174T cells. After treatment with Ac<sub>4</sub>ManLev for three days and subsequent incubation with A488-hydrazide for 30 min, LS174T cells were transferred to fresh medium and imaged under a fluorescence microscope to monitor the sub-cellular location of A488 signal. At the beginning of incubation, a strong A488 fluorescence signal was detected on the cell membrane, as evidenced by the overlay of A488 signal and cell membrane stain (Fig. 2c), indicating the successful conjugation of A488-hydrazide to cell-surface ketone groups. At 6 h, a large portion of A488 signal co-localized with Lysotracker™ Red DND-99, a stain for endosomes/lysosomes, indicating the entry of A488-labeled glycans into endosomes/lysosomes (Fig. 2c). Allowing for a longer time (12 h) for cellular internalization, more A488 signal appeared in endosomes/lysosomes (Fig. 2c). These experiments demonstrated that covalently conjugated

A488-hydrazide by cell-surface ketone groups was internalized and gradually entered endosomes, which is consistent with our previous findings on cellular internalization of DBCO-molecules by azido-labeled cells [8]. Upon conjugation with ketone-labeled glycans, a pH-responsive hydrazone linkage will be formed between the cargo and glycans, which can be potentially cleaved in acidic endosomes to release the pristine cargo.

We next studied whether the hydrazone bond between hydrazide and ketone-modified glycans can be cleaved in the acidic endosomes/lysosomes and whether the recovered ketone-modified glycans can be recycled to the cell membrane for repetitive targeting of hydrazide-molecule, using fluorescent A488-hydrazide and A647-hydrazide as examples (Fig. 3a). LS174T cells metabolically labeled with ketone groups, as achieved by Ac<sub>4</sub>ManLev pretreatment, were incubated with excessive A488-hydrazide for 1 h and transferred to fresh medium, followed by the addition of A647-hydrazide after 0, 6, 12, and 24 h, respectively. When A647-hydrazide was added immediately after A488-hydrazide conjugation, cells failed to capture A647-hydrazide, as evidenced by the minimal A647 signal on the cell membrane (Fig. 3b-c). A647-hydrazide that was added at 6 h post A488-hydrazide conjugation was successfully captured by cells, although only a small amount of A647 signal was detected on the cell surface (Fig. 3b-c). If A647-

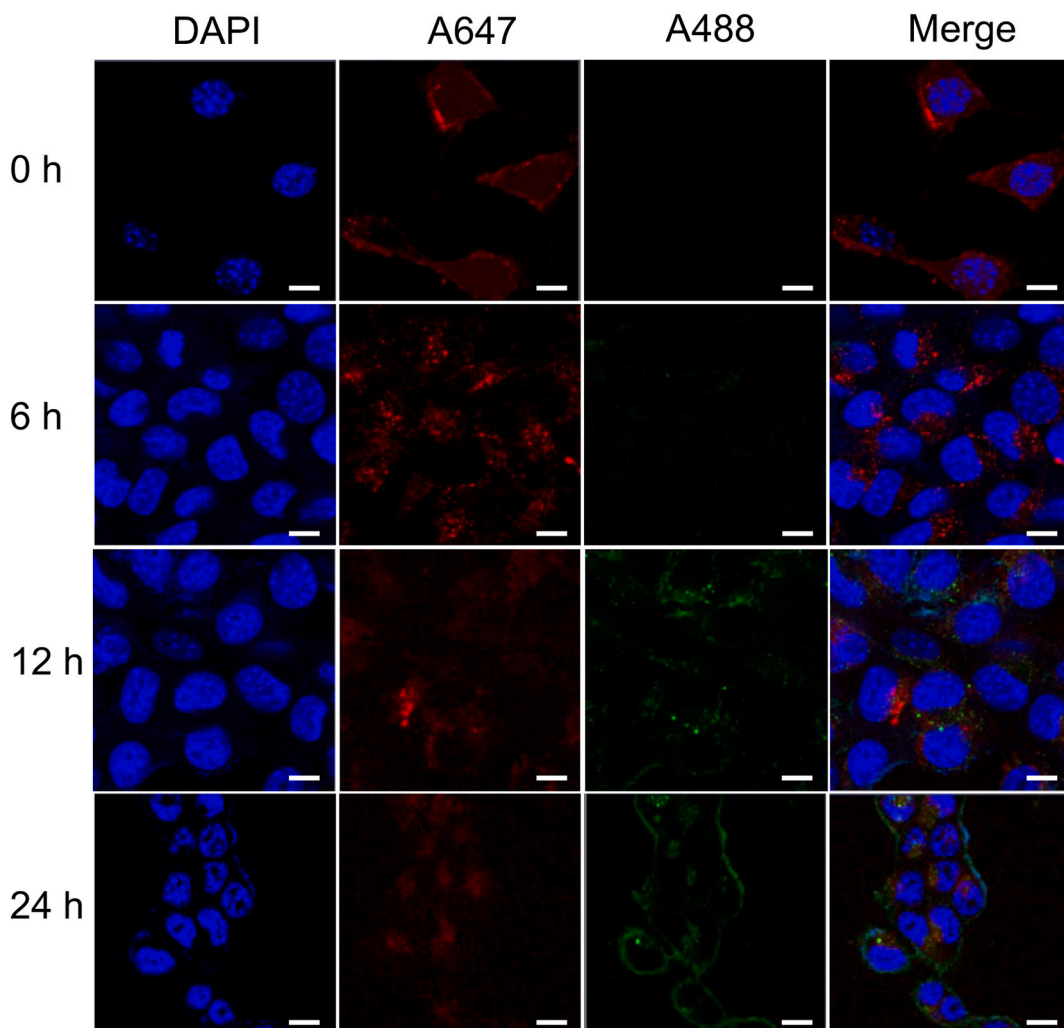


**Fig. 4.** Cell-surface ketone groups can be recycled after conjugation with A647-hydrazide, for subsequent targeting of A488-hydrazide. Shown are the confocal images of LS174T cells after 1-h incubation with A488-hydrazide that was added at 0, 6, 12, and 24 h, respectively post covalent capture of A647-hydrazide. Cells were pretreated with Ac<sub>4</sub>ManLev (100  $\mu$ M) for three days and incubated with A647-hydrazide for 1 h. After A647-hydrazide conjugation, cells were transferred to fresh medium and further incubated for 0, 6, 12, or 24 h prior to the addition of A488-hydrazide. Cell nuclei were stained with DAPI (blue). Scale bar: 10  $\mu$ m. (For interpretation of the references to colour in this figure legend, the reader is referred to the web version of this article.)

hydrazide was added at 12 h, the A488 signal nearly completely entered endosomes/lysosomes and a higher A647 fluorescence intensity was detected on the cell membrane (Fig. 3b-c). At 24 h post A488-hydrazide conjugation, cells could readily capture a significantly higher amount of A647-hydrazide (Fig. 3b-c). Flow cytometry analysis of LS174T cells confirmed an increased A647 signal when A647-hydrazide was added at 12 or 24 h post A488-hydrazide conjugation, in comparison to the addition of A647-hydrazide at 0 or 6 h post A488-hydrazide conjugation (Fig. 3c). By switching the order of A647-hydrazide and A488-hydrazide, a similar phenomenon was observed, i.e., A488-hydrazide that was added at 12 or 24 h post A647-hydrazide conjugation could be captured by ketone-labeled LS174T cells (Fig. 4). These experiments demonstrated that cell-surface ketone groups can be recycled after covalent capture of extracellular A488-hydrazide (or A647-hydrazide), for subsequent targeted conjugation of A647-hydrazide (or A488-hydrazide). It is noteworthy that a minimal amount of A647-hydrazide was conjugated to LS174T cells at 6 h post A488-hydrazide conjugation (Fig. 3b-c), indicating that it took some time for A647-conjugated glycans to escape from endosomes and become recycled to the cell membrane. While the exact rate of ketone recycling remains unknown and requires more accurate quantification of cell-surface ketone groups, the mean fluorescence intensity values extracted from FACS plots (Fig. 3c) indicated that ~20% and ~50% of targeting capacity can be recovered at 12 h and 24 h, respectively, post the first-round targeting.

In contrast, targeted delivery of cargo mediated by azide-dibenzocyclooctyne (DBCO) click chemistry is not reversible. At 12 h post incubation of azido-labeled LS174T cells with DBCO-Cy5, the added DBCO-FITC showed minimal targeting effect (Fig. 5), indicating that cell-surface azido groups were largely consumed by DBCO-Cy5 and could not be reversed. In addition to the targeting effect resulted from ketone-hydrazide chemistry, the ability to preferentially label cancer

cells with ketone groups is also critical for the development of cancer-targeted therapies. By pretreating LS174T cancer cells or IMR90 fibroblasts with Ac<sub>4</sub>ManLev or PBS for 72 h and then incubating with A488-hydrazide for 1 h, Ac<sub>4</sub>ManLev-pretreated LS174T cells showed significantly higher A488 fluorescence intensity compared to non-pretreated LS174T cells or Ac<sub>4</sub>ManLev-treated IMR90 cells (Fig. S5a-b). In contrast, Ac<sub>4</sub>ManLev-pretreated IMR90 cells showed similar A488 fluorescence intensity to non-pretreated IMR90 cells (Fig. S5a-b). The preferential labeling of cancer cells to healthy cells could be attributed to the much more active sugar metabolisms. The cancer-labeling selectivity can be further improved by modifying the C1 site of Ac<sub>4</sub>ManLev with a protecting group that can be removed in response to cancer-overexpressing enzymes, as we previously demonstrated [8].

After demonstrating that ketone-labeled cancer cells can mediate repetitive targeting of hydrazide molecules, we next studied whether metabolic labeling of cancer cells with ketone groups enables targeted conjugation of hydrazide-bearing therapeutics (Fig. 6a). An ideal hydrazide-bearing pro-drug should have lower toxicity than the unmodified drug, but can be degraded into the pristine drug molecule upon internalization by cancer cells. To this end, we reacted ketone-bearing doxorubicin (Dox) with a di-hydrazide molecule to yield a Dox-hydrazide conjugate with a hydrazone linkage between Dox and hydrazide (Fig. 6a, Fig. S6). Upon conjugation to ketone-labeled cancer cells, the Dox-hydrazide conjugate would be able to release pristine Dox in acidic endosomes (Fig. 6a). At pH 7.4, Dox-hydrazide was relatively stable, with a minimal release of Dox within 24 h (Fig. 6b). At pH 6.5, ~20% Dox was released over 24 h (Fig. 6b). The degradation rate was dramatically increased at pH 5.0 (Fig. 6b, Fig. S7), demonstrating the pH-responsiveness of Dox-hydrazide. To study whether ketone-labeled cancer cells can mediate conjugation of Dox-hydrazide, LS174T cells that were pretreated with Ac<sub>4</sub>ManLev or PBS for three days were

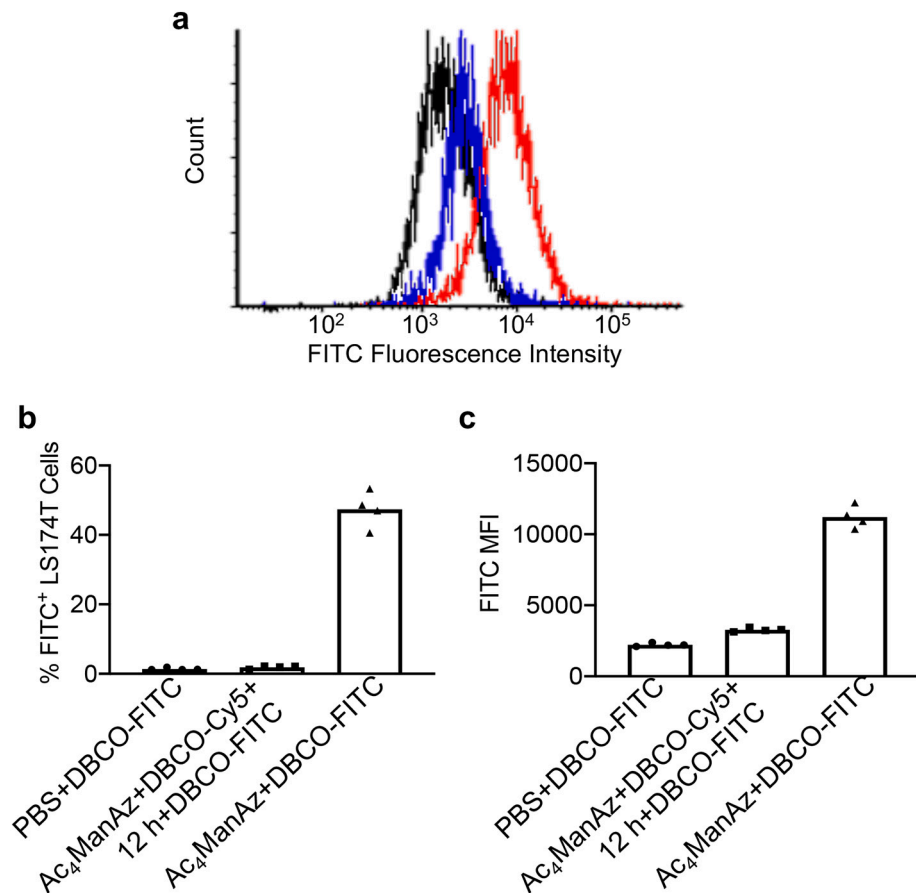
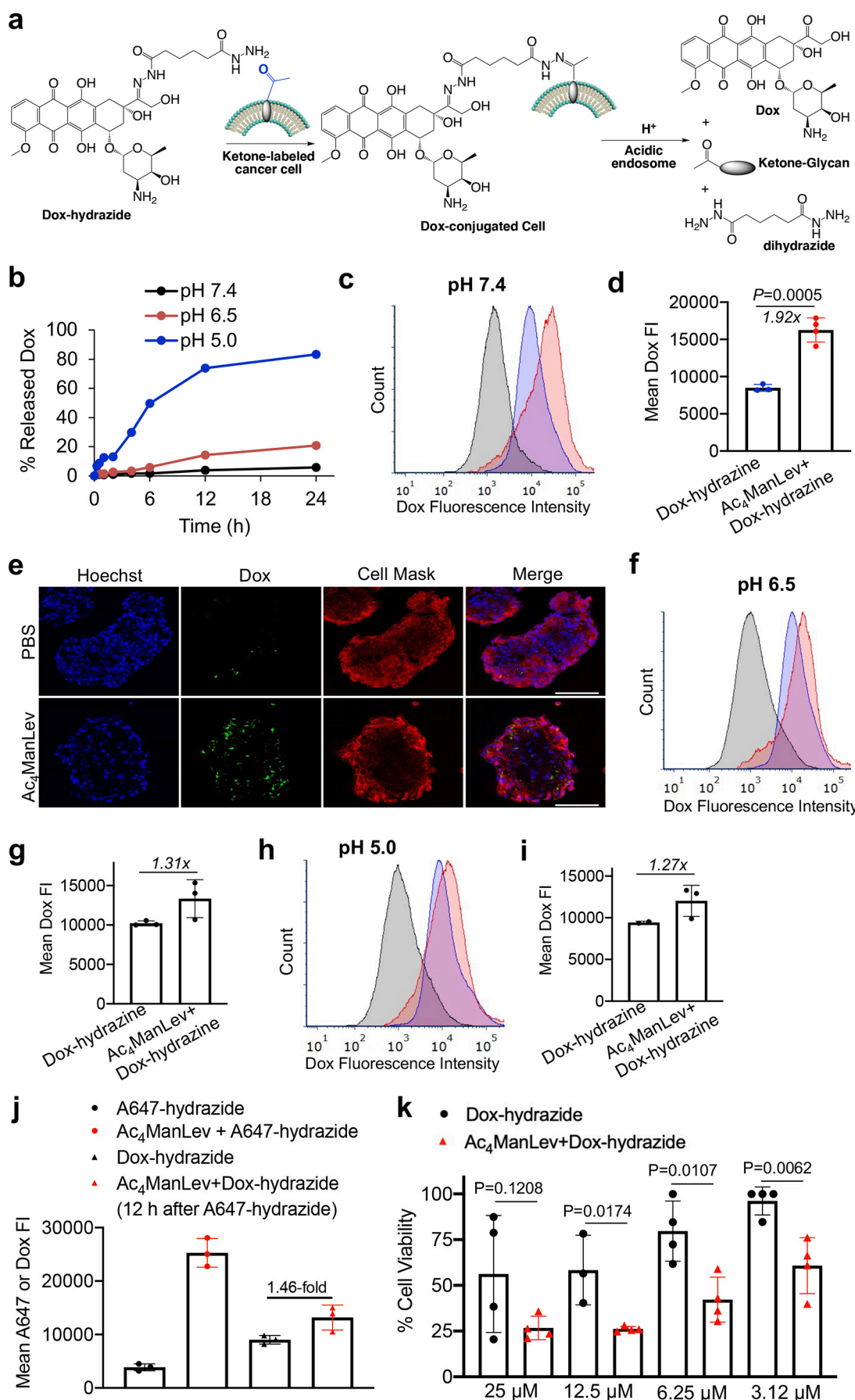


**Fig. 5.** Cell-surface azido groups cannot be recycled after covalent conjugation with DBCO-molecules. LS174T cells were pretreated with Ac<sub>4</sub>ManAz for three days and incubated with 10  $\mu$ M DBCO-Cy5 for 2 h at 37 °C. After DBCO-Cy5 conjugation, cells were transferred to fresh medium and further incubated for 12 h prior to the addition of 10  $\mu$ M DBCO-FITC for another 2 h. Cells were analyzed by flow cytometer where dead cells were excluded by a fixable cell viability dye. (a) Representative FITC histogram of LS174T cells treated with Ac<sub>4</sub>ManAz + DBCO-Cy5 + DBCO-FITC (blue). Cells pretreated with PBS for three days and incubated with DBCO-FITC were used as negative controls (black), and cells pretreated with Ac<sub>4</sub>ManAz and incubated with DBCO-FITC were used as positive controls (red). (b) Percentages of FITC<sup>+</sup> LS174T cells. (c) Mean FITC fluorescence intensity of cells for each group ( $n = 4$ ). All the numerical data are presented as mean  $\pm$  SD. (For interpretation of the references to colour in this figure legend, the reader is referred to the web version of this article.)



(caption on next page)

**Fig. 6.** Ketone-labeled cancer cells enable targeted conjugation of Dox-hydrazide. (a) Schematic illustration for the conjugation of Dox-hydrazide onto ketone-labeled cells and subsequent cleavage of the formed hydrazone bond to release Dox and ketone-glycans in acidic endosomes. (b) Degradation profiles of Dox-hydrazide at pH 7.4, 6.5, and 5.0, respectively, as determined by HPLC with a fluorescence detection channel. (c-i) LS174T cells were treated with Ac<sub>4</sub>ManLev for three days, and incubated with Dox-hydrazide for 1 h at pH 7.4 (c-e), 6.5 (f-g), and 5.0 (h-i), respectively. Dead cells were excluded during the flow cytometry analysis. (c, f, h) Representative histograms of LS174T cells treated with PBS (black), Dox-hydrazide only (blue), or Ac<sub>4</sub>ManLev + Dox-hydrazide (red), with Dox-hydrazide incubation performed at pH 7.4 (c), 6.5 (f), and 5.0 (h), respectively. (d, f, h) Mean Dox fluorescence intensity of LS174T cells treated with Dox-hydrazide only or Ac<sub>4</sub>ManLev + Dox-hydrazide, with Dox-hydrazide incubation performed at pH 7.4 (d), 6.5 (g), and 5.0 (i), respectively. (e) Representative confocal images of LS174T cells after 3-day treatment with PBS or Ac<sub>4</sub>ManLev and 1-h incubation with Dox-hydrazide at pH 7.4. The cell nucleus and membrane were stained with Hoechst 33342 (blue) and deep red Cell Mask (red), respectively. Scale bar: 100  $\mu$ m. (j) Mean A647 or Dox fluorescence intensity of Ac<sub>4</sub>ManLev-pretreated or non-pretreated LS174T cells after 1-h incubation with A647-hydrazide, 12-h incubation in a blank medium, and 1-h incubation with Dox-hydrazide. Dox fluorescence was detected via the PE-Texas Red channel. (k) Viability of Ac<sub>4</sub>ManLev-pretreated or non-pretreated LS174T cells after treatment with different concentrations (25, 12.5, 6.25, or 3.12  $\mu$ M) of Dox-hydrazide for 48 h. Ac<sub>4</sub>ManLev-pretreated or non-pretreated LS174T cells without Dox-hydrazide treatment were used as the controls for calculating the cell viability. All the numerical data are presented as mean  $\pm$  SD. (For interpretation of the references to colour in this figure legend, the reader is referred to the web version of this article.)

incubated with Dox-hydrazide at pH 7.4, 6.5, or 5.0, respectively, for 1 h. At pH 7.4, a significantly higher amount of Dox-hydrazide was detected in Ac<sub>4</sub>ManLev-pretreated cells compared to control cells without ketone labeling (Fig. 6c-d), indicating successful conjugation of Dox-hydrazide by ketone-labeled cells. Confocal imaging also confirmed the higher uptake of Dox-hydrazide by Ac<sub>4</sub>ManLev-pretreated LS174T cells compared to PBS-pretreated cells (Fig. 6e). At lower pH (6.5 or 5.0), a higher accumulation of Dox-hydrazide was still detected in Ac<sub>4</sub>ManLev-pretreated cells than in control cells (Fig. 6f-i). However, the fold-increase was lower at acidic pH (Fig. 6g, 6i), presumably due to the degradation of Dox-hydrazide during the 1-h incubation. These experiments demonstrated that Ac<sub>4</sub>ManLev can metabolically label cancer cells with ketone groups, for subsequent targeted conjugation of Dox-hydrazide. Upon internalization, pH-responsive Dox-conjugated glycans can release Dox and ketone-labeled glycans in acidic exosomes. The released Dox can induce the apoptosis and death of cancer cells (Fig. S8), while the released ketone-labeled sugars can be recycled for continuous targeting of hydrazide-bearing molecules. As Dox can induce the death of cancer cells and its fluorescence signal could alter intracellularly, comparing the total amount of Dox taken up by cells may not enable the validation of repetitive targeting of Dox-hydrazide. To address, we used A647-hydrazide for the first round of targeting, and then studied the targeting effect of Dox-hydrazide for the second round of targeting. Consistently, ketone-labeled LS174T cells mediated targeted conjugation of A647-hydrazide (Fig. 6j). At 12 h post conjugation of A647-hydrazide when ketone-sugars managed to recycle back to cell membranes, ketone-labeled LS174T cells showed significantly improved uptake of Dox-hydrazide compared to unlabeled LS174T cells (Fig. 6j). To investigate whether targeted conjugation of Dox-hydrazide could impart improved killing of cancer cells in vitro, LS174T cells with or without Ac<sub>4</sub>ManLev pretreatment were incubated with different concentrations (15, 12.5, 6.25, or 3.12  $\mu$ M) of Dox-hydrazide. At these concentrations, Dox-hydrazide showed the significantly improved killing of ketone-labeled LS174T cells compared to unlabeled LS174T cells (Fig. 6k). It is noteworthy that Ac<sub>4</sub>ManLev pretreatment itself did not cause significant cytotoxicity against LS174T cells (Fig. S9). We also studied the cytotoxicity of Dox-hydrazide (15 or 5  $\mu$ M) towards IMR90 fibroblasts with or without Ac<sub>4</sub>ManLev pretreatment, which all showed high viability after 48 h. Negligible differences in cell viability were detected between Ac<sub>4</sub>ManLev-pretreated and non-pretreated IMR90 cells (Fig. S10). These experiments demonstrated that metabolic labeling of cancer cells with ketone groups enables targeted conjugation of Dox-hydrazide for improved killing of cancer cells.

Metabolic glycan labeling provides a facile strategy to install unique chemical tags to cancer cell membranes, which can mediate targeted conjugation of diagnostic and therapeutic agents. However, the non-recyclability of cell-surface chemical tags (e.g., azide, alkene, cyclooctyne, etc.) after irreversible conjugation chemistries such as azide-DBCO chemistry could be a significant hurdle for developing effective cancer-targeted therapy. For example, azido-labeled cells can effectively covalently capture DBCO-agents via the formation of stable triazole

linkage, which irreversibly consumes the cell-surface azido groups and prevents further targeted conjugation of DBCO-agents (Fig. 5). The use of reversible chemistries can potentially address this issue. Using pH-responsive hydrazide-ketone reaction as an example, we showed that ketone-labeled cancer cells can covalently capture hydrazide-bearing cargo via a hydrazone linkage under neutral or mildly acidic pH. The conjugated agents are gradually internalized and enter endosomes/lysosomes within hours. As acidic late endosomes have a pH range of 5.0–6.0, the acid-labile hydrazone linkage between the cargo and ketone-modified glycans can be cleaved, potentially releasing ketone-labeled glycans from endosomes. These ketone-labeled glycans, once released from endosomes, could enter the recycling process and become re-expressed on the cell membrane, as demonstrated in our repetitive targeting experiment involving A488-hydrazide and A647-hydrazide (Fig. 3). Immediately after the covalent capture of A488-hydrazide, ketone-labeled LS174T cells showed minimal conjugation of A647-hydrazide, as a result of the consumption of cell-surface ketone groups by A488-hydrazide. Given more time to recycle ketone-modified glycans (12 or 24 h post conjugation of A488-hydrazide), cells were able to capture a significantly increased amount of A647-hydrazide compared to control cells (Fig. 3). The turn-over time, i.e. hours, is comparative to that of typical cell-surface protein receptors including G protein-coupled receptors (GPCRs) and estrogen receptors [35–37]. These experiments demonstrated that the use of reversible chemistries such as hydrazide/ketone reaction enables the recyclability of cell-surface chemical tags for repetitive targeting of diagnostic and therapeutic agents to cancer cells and other types of cells.

In order to achieve optimal cancer targeting in vivo, a fine balance between the reaction efficiency and reversibility is needed. While hydrazide/ketone reaction can occur in a neutral or mildly acidic microenvironment and is reversible in response to pH, the reaction efficiency is generally lower than the commonly used azide/DBCO or tetrazine/norbornene click chemistries [38–41]. Nevertheless, we observed  $> 5$ -fold increase of A488-hydrazide or A647-hydrazide conjugation and a 1.9-fold increase of Dox-hydrazide conjugation by ketone-labeled cells compared to the control cells at neutral pH (Fig. 2b, 3c, and 6c-e). The reaction rate of hydrazide-bearing cargo and ketone-labeled cells would increase under mildly acidic conditions [42], which may result in improved targeting of hydrazide-cargo. However, in the case of Dox-hydrazide, the existing hydrazone linkage between Dox and the ending hydrazide group made the conjugate unstable in an acidic medium. The replacement of the hydrazone linkage with another pH-irresponsive yet degradable linkage might enable a higher conjugation efficiency between hydrazide-bearing cargo and ketone-labeled cells in a mildly acidic condition such as the tumor microenvironment. Future development of new, highly efficient but reversible chemistries will also be of great value to fully exploit metabolic glycan labeling for cancer-targeted delivery of diagnostic and therapeutic agents.

### 3. Conclusion

To conclude, we describe a strategy to achieve recyclability of cell-surface chemical tags for repetitive targeted conjugation of agents. Using ketone/hydrazide chemistry as an example, Ac<sub>4</sub>ManLev can metabolically label cancer cells with ketone groups, which enable covalent capture of hydrazide-bearing agents via a degradable hydrazone linkage that can be cleaved in acidic endosomes. The released ketone-modified glycans can then be recycled to cell membranes for repetitive targeting of hydrazide-bearing agents. The ability to achieve repetitive targeting of therapeutic agents could be critical for achieving optimal anticancer efficacy, especially when different therapeutic agents need to be sequentially delivered to overcome drug resistance. In the case of immunotherapy, the ability to target a booster dose of immunomodulatory agents to cancerous tissues via the recyclable chemical tags would enable optimal amplification of anticancer immune responses. Future discovery of new reversible, efficient, and bio-orthogonal chemistries will further facilitate the application of metabolic glycan labeling to the development of potent cancer-targeted therapies.

### 4. Methods

#### 4.1. Materials and Instrumentation

D-Mannosamine hydrochloride, *N*-hydroxysuccinimidyl levulinate, and other chemical reagents were purchased from Sigma Aldrich (St. Louis, MO, USA) unless otherwise noted. Alexa Fluor 488-hydrazide, Alexa Fluor A647-hydrazide, eBioscience™ Fixable Viability Dye eFluor™ 780, and DBCO-FITC were purchased from ThermoFisher (Waltham, MA, USA). Doxorubicin was purchased from LC Laboratories (Woburn, MA, USA). CellMask™ Deep Red Plasma Membrane Stain and Lysotracker™ Red DND-99 were purchased from LC Laboratories (Woburn, MA, USA). DBCO-Cy5 was purchased from Click Chemistry Tools (Scottsdale, AZ, USA). FACS analyses were collected on Attune NxT or BD LSR Fortessa flow cytometers and analyzed on FlowJo v7.6 and FCS Express v6 and v7. Statistical testing was performed using GraphPad Prism v8. Small compounds were run on the Agilent 1290/6140 ultra-high-performance liquid chromatography/mass spectrometer or the Shimadzu high performance liquid chromatography. Proton nuclear magnetic resonance spectra were collected on the Agilent DD2 600. Confocal images were taken using the Upright Zeiss LSM 710 microscope. Preparative HPLC was performed on a CombiFlash®Rf system (Teledyne ISCO, Lincoln, NE, USA) equipped with a RediSep®Rf HP C18 column (Teledyne ISCO, 30 g, Lincoln, NE, USA). Lyophilization was conducted in a Labconco FreeZone lyophilizer (Kansas City, MO, USA).

#### 4.2. Cell line

The LS174T cell line was purchased from American Type Culture Collection (Manassas, VA, USA). Cells were cultured in DMEM containing 10% FBS, 100 units/mL Penicillin G and 100 µg/mL streptomycin at 37 °C in 5% CO<sub>2</sub> humidified air.

#### 4.3. Synthesis of tetraacetyl-*N*-(levulinic acyl)mannosamine (Ac<sub>4</sub>ManLev)

D-Mannosamine hydrochloride (2.5 mmol) and triethylamine (2.5 mmol) were dissolved in methanol, followed by the addition of *N*-hydroxysuccinimidyl levulinate (2.75 mmol). The mixture was stirred at room temperature for 24 h. Solvent was removed under reduced pressure and the residue was re-dissolved in pyridine. Acetic anhydride was added and the reaction mixture was stirred at room temperature for another 24 h. After removal of the solvent, the crude product was purified by silica gel column chromatography to yield a white solid (overall yield: 60%). <sup>1</sup>H NMR (500 MHz, CDCl<sub>3</sub>) δ 6.33 (d, *J* = 9.2 Hz, 1H), 5.84

(s, 1H), 5.09 (t, *J* = 9.5 Hz, 1H), 5.01 (dd, *J* = 9.7, 3.9 Hz, 1H), 4.73 (dd, *J* = 6.4, 4.9 Hz, 1H), 4.28 (dd, *J* = 12.4, 5.1 Hz, 1H), 4.15–3.94 (m, 1H), 3.79 (m, *J* = 6.6, 2.6 Hz, 1H), 2.90–2.69 (m, 2H), 2.58 (dt, *J* = 13.0, 6.3 Hz, 1H), 2.52–2.37 (m, 1H), 2.18–1.97 (m, 15H). <sup>13</sup>C NMR (CDCl<sub>3</sub>) δ 207.89, 173.04, 170.94, 170.28, 169.84, 168.79, 90.83, 73.53, 71.48, 65.49, 62.16, 49.39, 38.99, 30.21, 30.07, 21.02, 20.97, 20.90, 20.90. LRMS (*m/z*): [M + H]<sup>+</sup> calculated 446.4, detected 446.4; [2 M + H]<sup>+</sup> calculated 891.8, detected 891.8.

#### 4.4. General procedures for confocal imaging of ketone-labeled cells

LS174T cells were seeded onto coverslips in a 6-well plate at a density of 40 k cells per well and allowed to attach for 12 h. Ac<sub>4</sub>ManLev (100 µM) was added and the cells were incubated at 37 °C for 72 h. After washing with PBS, cells were incubated with Alexa Fluor 488-hydrazide (25 µM) in a medium (pH 7.4 or 6.5) for 30 min and fixed with a 4% PFA solution, followed by staining of cell nuclei with DAPI. The coverslips were mounted onto microscope slides and imaged under a confocal laser scanning microscope.

#### 4.5. General procedures for flow cytometry analysis of cells

LS174T cancer cells or IMR90 fibroblasts were seeded in a 24-well plate at a density of 20 k cells per well and allowed to attach for 12 h. Ac<sub>4</sub>ManLev (100 µM) was added and incubated with cells for 72 h. After washing with PBS, cells were incubated with Alexa Fluor 488-hydrazide or Alexa Fluor 647-hydrazide (25 µM) for 30 min. Cells were lifted by incubating with trypsin solution and analyzed by flow cytometry.

#### 4.6. Uptake mechanism of A488-hydrazide in Ac<sub>4</sub>ManLev treated cells

LS174T cells were seeded onto cell culture dishes with a cover glass bottom and incubated with Ac<sub>4</sub>ManLev (100 µM) for three days. After washing with PBS, the cells were incubated with Alexa Fluor 488-hydrazide (25 µM) and lysotracker green (2 µg/mL) for 30 min. Hoechst 33342 (10 µg/mL) and CellMask™ Deep Red Plasma membrane stain (1 µg/mL) were then added to stain cell nuclei and membrane, respectively, for 10 min. After washing with PBS, the cells were further incubated in a fresh medium at 37 °C for different times (0, 3, 6, 12, and 24 h) before being imaged under a fluorescence microscope to monitor the cellular internalization of Alexa Fluor 488-hydrazide.

#### 4.7. Uptake of A647-hydrazide in Ac<sub>4</sub>ManLev-treated cells post A488-hydrazide treatment

LS174T cells were seeded onto cell culture dishes with cover glass bottom and incubated with Ac<sub>4</sub>ManLev (100 µM) for three days. After washing with PBS, the cells were incubated with A488-hydrazide (50 µM) for 1 h. After washing with PBS, the cells were further incubated in a fresh medium at 37 °C for different times (0, 6, 12, and 24 h), at which time the medium was replaced with medium containing A647-hydrazide (50 µM) and the cells were further incubated for 1 h. Cells were then washed, fixed, stained with Hoechst 33342, and imaged under a confocal laser scanning microscope.

#### 4.8. Uptake of DBCO-FITC in Ac<sub>4</sub>ManAz-treated cells post DBCO-Cy5 treatment

LS174T cells were seeded in a 24-well plate at an initial density of 20 k cells per well and allowed to attach for 12 h. Ac<sub>4</sub>ManAz (50 µM) was added and incubated with cells for 72 h. After washing with PBS, cells were incubated with 10 µM DBCO-Cy5 for 2 h at 37 °C. Cells were then transferred to a fresh medium and cultured for another 12 h. After washing with PBS, 10 µM DBCO-FITC was added and incubated for another 2 h. Cells were lifted by trypsin, stained with a fixable viability dye, and fixed with 0.4% paraformaldehyde in PBS prior to flow

cytometry analysis.

#### 4.9. Synthesis of doxorubicin-hydrazide

Doxorubicin hydrochloride (0.1 mmol) and adipic acid dihydrazide (1.0 mmol) were dissolved in DMF, followed by addition of one drop of concentrated hydrochloric acid. The reaction mixture was stirred at 40 °C for 24 h. Dox-hydrazide was purified via preparative HPLC using water containing 5 mM NH<sub>4</sub>HCO<sub>3</sub> and acetonitrile as the mobile phases. Acetonitrile was removed under reduced pressure, and the residue was lyophilized to obtain a red solid (overall yield: 70%). MS (*m/z*): [M + H]<sup>+</sup> calculated 700.28, detected 700.28.

#### 4.10. pH-dependent degradation of doxorubicin-hydrazide

Doxorubicin-hydrazide (1 mg) was dissolved in 1 mL of PBS (2% DMSO) with a pH value of 5.0 or 6.5 or 7.4, and incubated at 37 °C with gentle shaking. At selected time points, 10 μL of Doxorubicin-hydrazide solution was injected into HPLC. The percentage of released Dox was determined via a standard curve of Dox.

#### 4.11. Conjugation of doxorubicin-hydrazide to ketone-labeled cancer cells

Cancer cells were seeded in 24-well plates with a density of 40 k per well. Cells were then treated with Ac<sub>4</sub>ManLev (100 μM) or PBS for three days. After washing, cells were further incubated with doxorubicin-hydrazide (100 μM) in cell media of different pH values (7.4, 6.5, or 5.0) for 1 h. After three washing steps, cells were lifted with trypsin and collected for flow cytometry analyses. To validate the repetitive targeting, LS174T cells pretreated with Ac<sub>4</sub>ManLev (100 μM) or PBS were first incubated with A647-hydrazide for 1 h, transferred to a blank medium for 12 h, and then incubated with doxorubicin-hydrazide (100 μM) for 1 h. Flow cytometry analysis of cells was performed to determine the cellular uptake of fluorescent A647 and doxorubicin.

#### 4.12. Confocal imaging of cells incubated with doxorubicin-hydrazide

LS174T cells were seeded in a 4-well chamber slide at a density of 50 k cells per well, and allowed to attach for 12 h. Ac<sub>4</sub>ManLev (50 μM) or PBS was added and the cells were incubated at 37 °C for 72 h. After washing with PBS twice, Dox-hydrazide (100 μM) was added to each well and cultured at 37 °C for 1 h. After washing with PBS, cells were incubated with Hoechst (1 μg/mL) for 10 min and CellMask Deep Red Plasma membrane (10 μg/mL) for 5 min. The slides were collected and fixed with 4% PFA solution. The coverslips were mounted onto microscope slides and imaged under a confocal laser scanning microscope.

#### 4.13. MTT study of doxorubicin-hydrazide and doxorubicin

In vitro cytotoxicity of doxorubicin-hydrazide and free doxorubicin was measured by MTT assay. LS174T colon cancer cells were seeded in a 96-well plate at an initial density of 4 k cells/well, allowed to attach for 24 h, and treated with doxorubicin-hydrazide or free doxorubicin at various concentrations at 37 °C for 48 h. Cells without drug treatment were used as control. The MTT assay was performed by following the standard procedure. MTT assay of Ac<sub>4</sub>ManLev was performed similarly except for the change of incubation time to 72 h. To study whether Ac<sub>4</sub>ManLev coupled with doxorubicin-hydrazide could improve the killing of cancer cells, LS174T cells were pretreated with Ac<sub>4</sub>ManLev (50 μM) or PBS for three days and then incubated with doxorubicin-hydrazide of varying concentrations (25, 12.5, 6.25, or 3.12 μM) for 48 h, prior to MTT assay. To study the cytotoxicity of doxorubicin-hydrazide to IMR90 fibroblasts, IMR90 cells were pretreated with Ac<sub>4</sub>ManLev (50 μM) or PBS for three days and then incubated with doxorubicin-hydrazide of varied concentrations (15 or 5 μM) for 48 h,

prior to MTT assay.

#### 4.14. Statistical analyses

Statistical analysis was performed using GraphPad Prism v6 and v8. Sample variance was tested using the F test. For samples with equal variance, the significance between the groups was analyzed by a two-tailed student's *t*-test. For samples with unequal variance, a two-tailed Welch's *t*-test was performed. For multiple comparisons, a one-way analysis of variance (ANOVA) with post hoc Fisher's LSD test was used. The results were deemed significant at 0.01 < \**P* ≤ 0.05, highly significant at 0.001 < \*\**P* ≤ 0.01, and extremely significant at \*\*\**P* ≤ 0.001.

#### Data availability

Raw data can be accessed upon request, and will be published upon the acceptance of the manuscript.

#### CRediT authorship contribution statement

**Rimsha Bhatta:** Investigation, Methodology, Formal analysis, Writing – review & editing. **Joonsu Han:** Investigation, Methodology, Formal analysis, Writing – review & editing. **Jingyi Zhou:** Investigation, Writing – review & editing. **Haoyu Li:** Investigation. **Hua Wang:** Conceptualization, Supervision, Formal analysis, Writing – review & editing.

#### Declaration of Competing Interest

The authors declare no competing financial interests.

#### Acknowledgements

The authors would like to acknowledge the financial support from NSF CAREER DMR-2143673 and the start-up package from the Department of Materials Science and Engineering at the University of Illinois at Urbana-Champaign and the Cancer Center at Illinois.

#### Appendix A. Supplementary data

Supplementary data to this article can be found online at <https://doi.org/10.1016/j.jconrel.2022.05.007>.

#### References

- [1] Y.H. Xie, Y.X. Chen, J.Y. Fang, *Signal Transduction and Targeted Therapy* 5 (2020) 1–30.
- [2] A.M. Scott, J.D. Wolchok, L.J. Old, *Nat. Rev. Cancer* 12 (2012) 278–287.
- [3] D. Schrama, R.A. Reisfeld, J.C. Becker, *Nat. Rev. Drug Discov.* 5 (2006) 147–159.
- [4] J.Y. Li, S.R. Perry, V. Muniz-Medina, X. Wang, L.K. Wetzel, M.C. Rebelatto, M.J. M. Hinrichs, B.Z. Bezabeh, R.L. Fleming, N. Dimasi, *Cancer Cell* 29 (2016) 117–129.
- [5] M.X. Sliwkowski, I. Mellman, *Science* 341 (2013) 1192–1198.
- [6] J.M. Baskin, J.A. Prescher, S.T. Laughlin, N.J. Agard, P.V. Chang, I.A. Miller, A. Lo, J.A. Codelli, C.R. Bertozzi, *Proc. Natl. Acad. Sci.* 104 (2007) 16793–16797.
- [7] P.V. Chang, J.A. Prescher, E.M. Sletten, J.M. Baskin, I.A. Miller, N.J. Agard, A. Lo, C.R. Bertozzi, *Proc. Natl. Acad. Sci.* 107 (2010) 1821–1826.
- [8] H. Wang, R. Wang, K. Cai, H. He, Y. Liu, J. Yen, Z. Wang, M. Xu, Y. Sun, X. Zhou, Q. Yin, L. Tang, I.T. Dobrucki, L.W. Dobrucki, E.J. Chaney, S.A. Boppart, T.M. Fan, S. Lezmi, X. Chen, L. Yin, J. Cheng, *Nat. Chem. Biol.* 13 (2017) 415.
- [9] S.T. Laughlin, N.J. Agard, J.M. Baskin, I.S. Carrico, P.V. Chang, A.S. Ganguli, M. J. Hangauer, A. Lo, J.A. Prescher, C.R. Bertozzi, *Methods Enzymol.* 415 (2006) 230–250.
- [10] S.J. Luchansky, S. Goon, C.R. Bertozzi, *ChemBioChem* 5 (2004) 371–374.
- [11] K.J. Yarema, L.K. Mahal, R.E. Bruehl, E.C. Rodriguez, C.R. Bertozzi, *J. Biol. Chem.* 273 (1998) 31168–31179.
- [12] S.T. Laughlin, C.R. Bertozzi, *Nat. Protoc.* 2 (2007) 2930.
- [13] J.A. Prescher, D.H. Dube, C.R. Bertozzi, *Nature* 430 (2004) 873–877.
- [14] H. Wang, D.J. Mooney, *Nat. Chem.* 12 (2020) 1102–1114.
- [15] H. Wang, L. Tang, Y. Liu, I.T. Dobrucka, L.W. Dobrucki, L. Yin, J. Cheng, *Theranostics* 6 (2016) 1467–1476.

[16] H. Wang, Y. Bo, Y. Liu, M. Xu, K. Cai, R. Wang, J. Cheng, *Biomaterials* 218 (2019), 119305.

[17] H. Wang, M. Gauthier, J.R. Kelly, R.J. Miller, M. Xu, W.D. O'Brien Jr., J. Cheng, *Angew. Chem. Int. Ed.* 55 (2016) 5452–5456.

[18] H. Wang, Y. Liu, M. Xu, J. Cheng, *Biomaterials Science* (2019), <https://doi.org/10.1039/C9BM00898E>.

[19] H. Koo, S. Lee, J.H. Na, S.H. Kim, S.K. Hahn, K. Choi, I.C. Kwon, S.Y. Jeong, K. Kim, *Angew. Chem. Int. Ed.* 51 (2012) 11836–11840.

[20] M.K. Shim, H.Y. Yoon, J.H. Ryu, H. Koo, S. Lee, J.H. Park, J.H. Kim, S. Lee, M. G. Pomper, I.C. Kwon, *Angew. Chem. Int. Ed.* 55 (2016) 14698–14703.

[21] S. Lee, H. Koo, J.H. Na, S.J. Han, H.S. Min, S.J. Lee, S.H. Kim, S.H. Yun, S.Y. Jeong, I.C. Kwon, K. Choi, K. Kim, *ACS Nano* 8 (2014) 2048–2063.

[22] S. Lee, S. Jung, H. Koo, J.H. Na, H.Y. Yoon, M.K. Shim, J. Park, J.-H. Kim, S. Lee, M. G. Pomper, I.C. Kwon, C.-H. Ahn, K. Kim, *Biomaterials* 148 (2017) 1–15.

[23] R. Xie, L. Dong, Y. Du, Y. Zhu, R. Hua, C. Zhang, X. Chen, *Proc. Natl. Acad. Sci.* 113 (2016) 5173–5178.

[24] R. Xie, L. Dong, R. Huang, S. Hong, R. Lei, X. Chen, *Angew. Chem. Int. Ed.* 53 (2014) 14082–14086.

[25] R. Wang, K. Cai, H. Wang, C. Yin, J. Cheng, *Chem. Commun.* 54 (2018) 4878–4881.

[26] B.D. Grant, J.G. Donaldson, *Nat. Rev. Mol. Cell Biol.* 10 (2009) 597–608.

[27] S.L. Bowman, D.J. Shiawski, M.A. Putthenveedu, *J. Cell Biol.* 214 (2016) 797–806.

[28] V.W. Hsu, M. Bai, J. Li, *Nat. Rev. Mol. Cell Biol.* 13 (2012) 323–328.

[29] K.R. West, S. Otto, *Current Drug Discovery Technologies* 2 (2005) 123–160.

[30] S.J. Sonawane, R.S. Kalhapure, T. Govender, *Eur. J. Pharm. Sci.* 99 (2017) 45–65.

[31] N. Deirram, C. Zhang, S.S. Kermanian, A.P. Johnston, G.K. Such, *Macromol. Rapid Commun.* 40 (2019) 1800917.

[32] M. Kanamala, W.R. Wilson, M. Yang, B.D. Palmer, Z. Wu, *Biomaterials* 85 (2016) 152–167.

[33] D.A. Nauman, C.R. Bertozzi, *Biochimica et Biophysica Acta (BBA)-General Subjects* 1568 (2001) 147–154.

[34] L.K. Mahal, K.J. Yarema, C.R. Bertozzi, *Science* 276 (1997) 1125–1128.

[35] C.C. Valley, N.M. Solodin, G.L. Powers, S.J. Ellison, E.T. Alarid, *J. Mol. Endocrinol.* 40 (2008) 23–34.

[36] A.J.L. Clark, L. Chan, *Front. Endocrinol.* (2019) 10.

[37] H. Kumagai, Y. Ikeda, Y. Motozawa, M. Fujishiro, T. Okamura, K. Fujio, H. Okazaki, S. Nomura, N. Takeda, M. Harada, H. Toko, E. Takimoto, H. Akazawa, H. Morita, J.-i. Suzuki, T. Yamazaki, K. Yamamoto, I. Komuro, M. Yanagisawa, *PLoS One* 10 (2015), e0129394.

[38] J. Dommerholt, O. van Rooijen, A. Borrman, C.F. Guerra, F.M. Bickelhaupt, F. L. van Delft, *Nat. Commun.* 5 (2014) 5378.

[39] J. Dommerholt, F.P.J.T. Rutjes, F.L. van Delft, *Top. Curr. Chem.* 374 (2016) 16.

[40] A.V.B. de Oliveira, V. Kartnaller, C. Costa Neto, J. Cajaiba, *ACS Omega* 4 (2019) 13530–13537.

[41] D.K. Kölmel, E.T. Kool, *Chem. Rev.* 117 (2017) 10358–10376.

[42] E.T. Kool, D.-H. Park, P. Crisalli, *J. Am. Chem. Soc.* 135 (2013) 17663–17666.